RESEARCH

Potent telomerase activators from a novel sapogenin via biotransformation utilizing *Camarosporium laburnicola*, an endophytic fungus

Melis Küçüksolak[1], Sinem Yılmaz[2,3], Petek Ballar-Kırmızıbayrak[4] and Erdal Bedir[1*]

Abstract

Background Cycloartane-type triterpenoids possess important biological activities, including immunostimulant, wound healing, and telomerase activation. Biotransformation is one of the derivatization strategies of natural products to improve their bioactivities. Endophytic fungi have attracted attention in biotransformation studies because of their ability to perform modifications in complex structures with a high degree of stereospecificity.

Results This study focuses on biotransformation studies on cyclocephagenol (**1**), a novel cycloartane-type sapogenin from *Astragalus* species, and its 12-hydroxy derivatives (**2** and **3**) to obtain new telomerase activators. Since the hTERT protein levels of cyclocephagenol (**1**) and its 12-hydroxy derivatives (**2** and **3**) on HEKn cells were found to be notable, biotransformation studies were carried out on cyclocephagenol and its 12-hydroxy derivatives using *Camarosporium laburnicola*, an endophytic fungus isolated from *Astragalus angustifolius*. Later, immunoblotting and PCR-based ELISA assay were used to screen starting compounds and biotransformation products for their effects on hTERT protein levels and telomerase activation. All compounds showed improved telomerase activation compared to the control group.

Conclusions As a result of biotransformation studies, seven new metabolites were obtained and characterized, verifying the potential of *C. laburnicola* as a biocatalyst. Additionally, the bioactivity results showed that this endophytic biocatalyst is unique in transforming the metabolites of its host to afford potent telomerase activators.

Keywords Biotransformation, Endophytic Fungi, Sapogenin, Telomerase activator, Anti-aging

*Correspondence:
Erdal Bedir
erdalbedir@iyte.edu.tr
[1]Department of Bioengineering, Izmir Institute of Technology, Urla 35430, İzmir, Türkiye, Turkey
[2]Department of Biotechnology, Graduate School of Natural and Applied Sciences, Ege University, Bornova, İzmir, Türkiye, Turkey
[3]Department of Bioengineering, Faculty of Engineering, University of Alanya Aladdin Keykubat, Antalya, Türkiye, Turkey
[4]Department of Biochemistry, Faculty of Pharmacy, Ege University, Bornova 35100, İzmir, Türkiye, Turkey

Background

Modification of natural products occurs either by chemical reactions or by biotransformation reactions. Biotransformation is the biochemical reactions of living systems or their components (enzymes) to alter molecules. It is an effective tool in obtaining molecules that are difficult to prepare by conventional synthetic methods and has a wide range of uses. In the pharmaceutical industry, microbial biotransformation has been utilized in the enzymatic transformation to synthesize chiral intermediates and end products [1–4].

There are many applications of biotransformation in drug discovery and development studies, including the synthesis of drug metabolites for estimation of mammalian metabolism, lead optimization, and the development of metabolite libraries from highly diverse lead compounds for structure-activity relationship (SAR) and bioactivity screening studies [5]. In addition to overcoming the difficulties encountered in chemical synthesis, microbial biotransformation is effectively used to increase/reduce the bioactivity/toxicity profiles of drug precursor molecules and to generate molecular libraries for structure-activity studies with their highly diverse enzyme systems [3, 6–9].

Cycloartane-type triterpenoids are produced only by photosynthetic eukaryotes. In the plant kingdom, these metabolites are not as common as other triterpenoids (oleanane, ursane, steroidal triterpenoids). The plants richest in cycloartane-type of compounds are *Astragalus* species [10]. Nearly 650 cycloartane-type metabolites were identified, and almost half were obtained from *Astragalus* species [11, 12]. The biological activities of cycloartanes and their semi-synthetic derivatives indicate their wide range of bioactivities, including immunostimulant [13–15], anti-protozoal [16], antiviral [17], cytotoxic [18, 19], cardiotonic [20], wound healing [21] and adjuvant [22–24] activities. The most important development in the last ten years for cycloartanes was the discovery of cycloastragenol as a potent telomerase activator [25]. Since 2007, cycloastragenol, present only in *Astragalus* species, has been in the market as an anti-aging dietary supplement with the trade name TA-65.

Telomeres are specialized structures consisting of TTAGGG tandem repeat sequences at the ends of chromosomes. They protect chromosome ends from fusion and degradation and shorten over time in dividing somatic cells [26–28]. Telomerase is a cellular "reverse transcriptase" (TERT, telomerase reverse transcriptase) enzyme that uses the relevant RNA component (Terc, telomerase RNA component) as a template and helps repair telomere ends by adding TTAGGG repeats [29].

Telomerase activation is a potential target for treating diseases associated with telomere loss, as telomere shortening results from the biological aging process and is also considered a risk factor for many age-related diseases. In addition, conditions associated with telomere shortening are not only age-related. Hence, telomerase activation *in vivo* has significant potential for treating many chronic and degenerative diseases [30–35].

Cycloastragenol and its derivatives have been at the center of nature-based regenerative medicine research as well its utilization in degenerative diseases is a hot topic [30–34, 36]. Also, the entry of cycloastragenol and its derivatives into clinical trials for Alzheimer's disease (NCT number: 02531334) and metabolic syndrome (NCT number: 02530255) is an indication of the potential of telomerase activators toward degenerative diseases. In 2022, two new clinical studies were initiated using *Astragalus membranaceus* in cognitive impairment and parkinsonism (NCT number: 05578443 and 05506891, respectively).

In our previous studies, biotransformation studies were carried out on cycloartanes using endophytic fungi isolated from the tissues of *Astragalus* species, and the effects of the metabolites on telomerase activation were investigated. Cycloastragenol, cyclocanthogenol, and semi-synthetic derivatives astragenol and 20(27)-octanor cycloastragenol, the main triterpenoids in *Astragalus*, were used as starting molecules. In the telomerase activation screening panel using obtained metabolites, 16 compounds showed activity ranging from 1.2 to 11.3-fold at doses of 0.5 to 300 nM compared to the control cells treated with DMSO [37–39]. The significant modifications leading to the increase in activity were the oxidation of C-3(OH), conversion of ring A to 7-membered lactone, and the formation of 3(4)-seco structures via cleavage of the ring A, catalyzed by *Camarosporium laburnicola*. Another substantial modification was the hydroxylation of C-12 by the P450 monooxygenase system of *Alternaria eureka*.

Cyclocephagenol (**1**) is another major sapogenin in Turkish *Astragalus* species with a tetrahydropyran side chain in the cycloartane skeleton. In a recent study, we modified this sapogenin using *Alternaria eureka* to obtain new neuroprotective agents. As a result, potent metabolites exhibited bioactivities at the nanomolar range [40]. However, bioactivities of **1** or its conceivably effective metabolites (**2** and **3**: 12-hydroxy derivatives) on telomerase activation have never been screened. To see the potential of these compounds (**1–3**) towards telomerase activation, first, hTERT (human Telomerase Reverse Transcriptase) protein expression levels were evaluated. All compounds increased hTERT protein expression; therefore, we decided to perform a modification study on these compounds utilizing *C. laburnicola*, a well-proven biocatalyst to afford bioactive metabolites [37–39]. Later, we screened biotransformation products for their effects

on telomerase activation by immunoblotting and PCR-based ELISA assay.

Results

Effect of cyclocephagenol (1), 12α-hydroxycyclocephagenol (2), and 12β-hydroxycyclocephagenol (3) on hTERT expression

As hTERT protein level is a preliminary indicator of probable telomerase activation, compounds **1**, **2**, and **3** were screened for their effects on hTERT expression by Western Blot. All three metabolites were found to increase the hTERT protein levels compared to the DMSO-treated control group. While **1** and **3** increased the hTERT protein levels in a dose dependent-manner, metabolite **2** enhanced hTERT protein levels at 10, 30, and 100 nM concentrations (Fig. 1).

Based on the promising activities of these metabolites, biotransformation studies on **1**, **2**, and **3** were carried out to enrich our molecule library to obtain potent telomerase activators and investigate structure-activity relationships.

Biotransformation of cyclocephagenol (1) and 12α-hydroxycyclocephagenol (2) by *Camarosporium laburnicola*

The biotransformation of cyclocephagenol with the endophytic fungus *C. laburnicola* for four days afforded three metabolites (**4–6**), while the biotransformation studies performed on 12α-hydroxycyclocephagenol by *C. laburnicola* for 30 days yielded four metabolites (**7–10**) (Fig. 2). In the case of 12β-hydroxycyclocephagenol (**3**), metabolite production was relatively low. No further attempt was made to isolate its metabolites.

The structures of the compounds were established by 1D-, 2D-NMR, and HR-MS analyses. Comparison of the NMR data for **4–6** with those of **1** and **7–10** with those of **2** revealed the presence of the same partial structures for the B → E rings [40]. These observations suggested that A ring biotransformation occurred in metabolites **4–10**. For metabolites **7–10**, α-hydroxylation at C-12 was confirmed using 1D- and 2D-NMR spectra of these compounds.

HR-ESI-MS spectrum of **4** showing a major ion peak at *m/z* 545.34691 ([M+Na]$^+$) indicated a molecular formula of $C_{30}H_{50}O_7$. In the ^{13}C-NMR spectrum, the oxymethine signal belonging to C-3 was lost, and a carboxyl signal was deduced from δ_C 176.0 resonance. In addition, a quaternary carbon adjacent to oxygen (δ_C 75.7) was noticed. When five out of six degrees of unsaturation accounted for the ring systems (rings B → E and the cyclopropane) was assessed with the presence of a carboxyl group, revealing an additional unsaturation, a cleavage for ring A was evident. In the HMBC spectrum, the long-distance correlations from H-5, H$_3$-28, and H$_3$-29 to δ_C 75.7 justified the hydroxylation at C-4. Additionally, a downfield shift of H$_2$-2 signals (δ_H 2.96, m, H-2a; δ_C 2.60, m, H-2b) and the long-distance correlations from H-2 and H-1 to the carboxyl signal proved the structure being 3(4)-seco-cyclocephagenol. Based on these results, the structure of **4** was established as 20,25-epoxy-6α,16β,24α-trihydroxy-3,4-secocycloartan-3-oic acid.

The molecular formula of **5** was established as $C_{30}H_{48}O_6$ by HR-ESI-MS analysis (*m/z* 527.33635 [M+Na]$^+$). From detailed inspection of 1D- and 2D-NMR spectra, long-range correlations from two methylene groups (H$_2$-2 and H$_2$-1) to the carbonyl signal at 174.3 ppm suggested a ring opening for **5** at first glance, as in **4**. However, an oxygenated carbon was observed at 85.6 ppm in the ^{13}C-NMR spectrum. In the HMBC spectrum, long-range correlations from two methyl groups (δ_H 1.71 and 1.49) to δ_C 85.6 implied that it was C-4. The downfield shift of C-4 resonance (9.9 ppm) compared to metabolite **4** (δ_C 75.7) and previously reported metabolites of our group ascertained that C-4 was in a 7-membered lactone ring system [38, 41]. As a result, **5** was elucidated as 20,25-epoxy-6α,16β,24α-trihydroxycycloartan-3-olide.

The metabolite **6** gave a molecular formula of $C_{30}H_{48}O_5$ based on the HR-ESI-MS data (*m/z* 511.33940 [M+Na]$^+$). Apart from the oxymethine signals of C-3, the characteristic signals of the starting molecule **1** were present for **6**. In the ^{13}C-NMR spectrum, the resonance at 216.6 ppm was obvious, implying a biotransformation of C-3 secondary alcohol to a ketone via an oxidation reaction. Accordingly, this assumption was substantiated by long-range correlations between H-5/H$_3$-28/H$_3$-29 and C-3 (δ_C 216.6) in the HMBC spectrum. As a result, the structure of **6** was determined to be 20,25-epoxy-6α,16β,24α-trihydroxycycloartan-3-one.
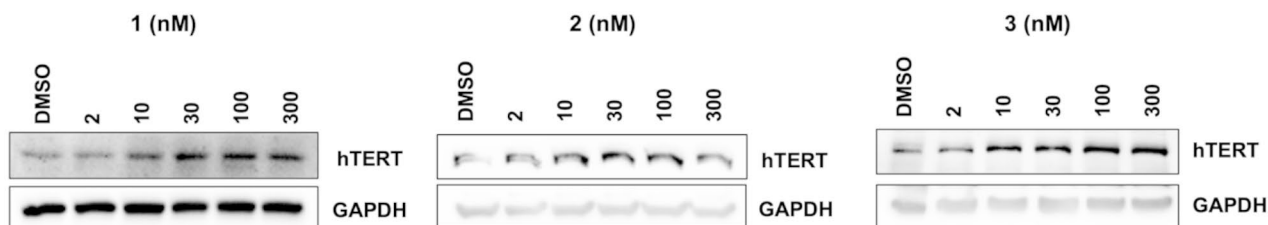

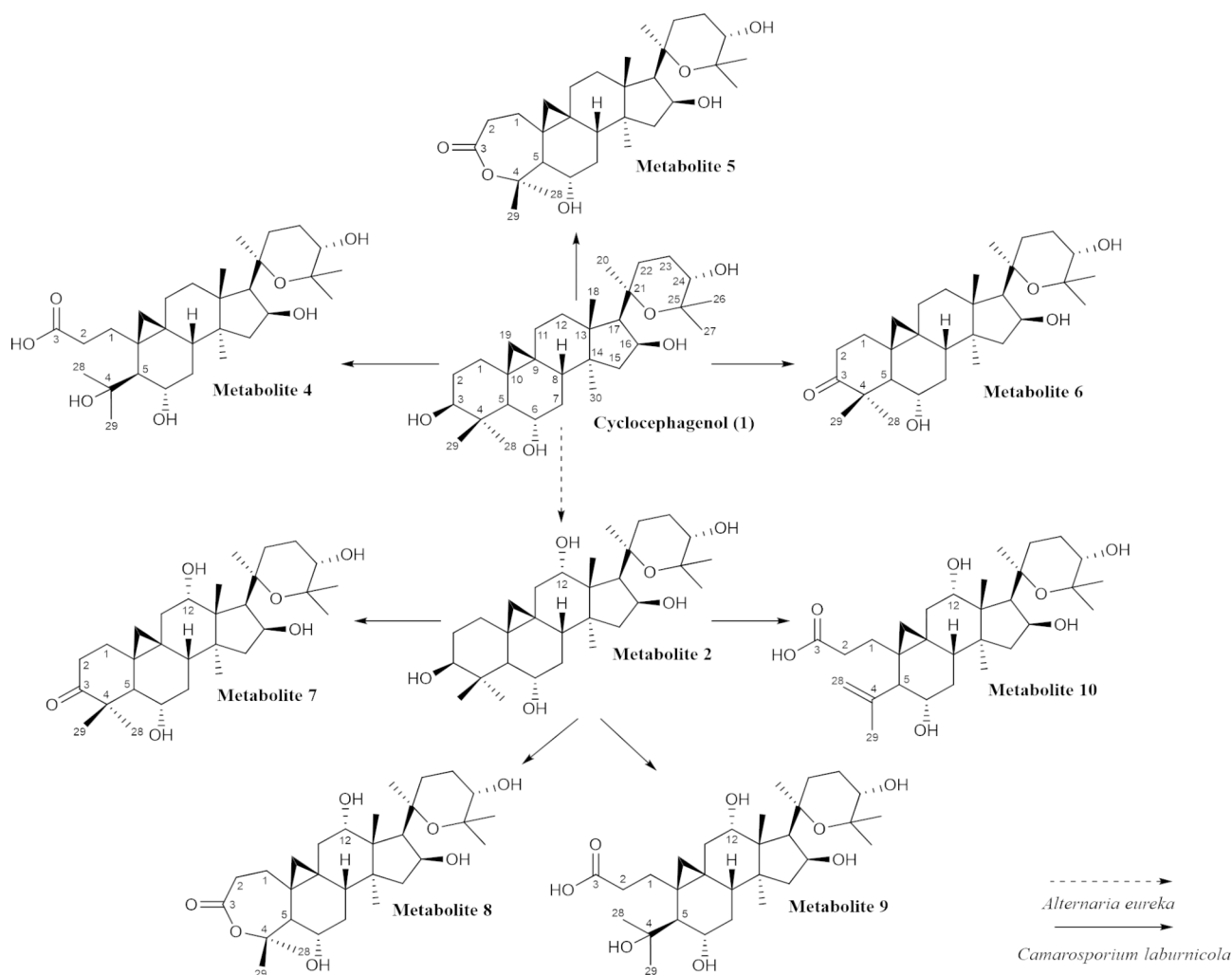**Fig. 1** Effects of **1**, **2**, and **3** on hTERT protein level

Fig. 2 Biotransformation products of **1** and **2** by *Camarosporium laburnicola*

The metabolite **7**, the first metabolite of **2** (12α-hydroxycyclocephagenol), gave a molecular formula of $C_{30}H_{48}O_6$ based on the HR-ESI-MS data (*m/z* 503.33835 [M - H]⁻). Apart from the proton and carbon resonances deriving from ring A, the characteristic signals of **2** were present for **7**. In the ^{13}C-NMR spectrum, the resonance at 217.4 ppm was obvious, implying a biotransformation of C-3 secondary alcohol to a ketone as in **6**. The long-range HMBC correlations from H-2b, H₃-28, and H₃-29 (δ_H 2.43, 1.78, and 1.50, respectively) to C-3 (δ_C 217.4) verified the oxidation location. As a result, the structure of **7** was determined to be 20,25-epoxy-6α,12α,16β,24α-tetrahydroxycycloartan-3-one.

The HR-ESI-MS spectrum of **8** showed a major ion peak at *m/z* 519.33289 [M - H]⁻ ($C_{30}H_{48}O_7$). Initial inspection of the ^1H-NMR spectrum of **8** revealed the absence of characteristic H-3 resonance. The HMBC spectrum showed a cross-peak between the H-1a signal (δ_H 1.42) and a carbonyl carbon at 173.6 ppm. From inspection of the ^{13}C-NMR and HMBC spectra, the

long-range correlations of two methyl groups (δ_H 1.94 and 1.70) and H-5 (δ_H 2.44) with an oxygenated carbon at δ_C 85.3 was observed. Thus, the resonance of δ_C 85.3 was readily assigned to C-4. Comparing the chemical shifts and coupling constants with those of **5**, it was ascertained that **8** also had a 7-membered lactone ring system in ring A. As a result, **8** was elucidated as 20,25-epoxy-6α,12α,16β,24α-tetrahydroxycycloartan-3-olide.

HR-ESI-MS spectrum of **9** showing a major ion peak at *m/z* 537.34344 ([M - H]⁻) indicated a molecular formula of $C_{30}H_{50}O_8$. In the ^{13}C-NMR spectrum, the oxymethine signal belonging to C-3 was lost, and a carboxyl signal was deduced from δ_C 179.5 resonance. In the HMBC spectrum, H₂-1 displayed cross-peaks with the carboxyl signal at δ_C 179.5, confirming the presence of the carboxyl group at C-3. In addition, a low-field carbon adjacent to oxygen (δ_C 76.4) was noticed. In the HMBC spectrum, the long-distance correlations from H-5, H₃-28 and H₃-29 to δ_C 76.4 helped us to assign it as C-4. These data implied a ring cleavage in ring A, as

in **4**. The resemblance of the spectral data of **9**, deduced from 1D- and 2D-NMR spectra, with those of **4** and **2** was evident for the characteristic 3(4)-seco structure with a carboxyl group at C-3 and hydroxyl functionality at C-4 establishing the structure of **4**. Based on these results, the structure of **9** was established as 20,25-epoxy-6α,12α,16β,24α-tetrahydroxy-3,4-secocycloartan-3-oic acid.

In the HR-ESI-MS spectrum of **10**, the major ion peak at *m/z* 519.33122 [M - H]$^-$ confirmed the molecular formula as $C_{30}H_{48}O_7$. The ^1H and ^{13}C-NMR spectra of **10** implied a ring cleavage as in compound **9**. The resonances observed at δ_H 5.21 and 5.09 suggested an exocyclic methylene group corresponding to carbon at δ_C 115.3 in the HSQC spectrum. In addition, one of the two methyl groups at C-4 disappeared, and the other shifted to a low field (δ_{H-29} 1.89). The HMBC spectrum displayed cross-peaks from H_3-29 (δ_H 1.89) to C-28 (δ_C 115.3), C-4 (δ_C 147.1), and C-5 (δ_C 55.7). This indicated that an A-ring cleavage was followed by a dehydration reaction yielding a C-4(28) disubstituted double bond system. Accordingly, the ^1H-^1H COSY spectrum revealed a spin system of H-28a (δ_H 5.21) → H-28b (δ_H 5.09) → H_3-29 (δ_H 1.89) and justifying this assignment. Unexpectedly, the cross-peaks from H_2-1 and H_2-2 to the carboxyl carbon at δ_C 177.3 was not noticeable in the HMBC spectrum. Nevertheless, resemblance of the spectral data of **10**, deduced from 1D- and 2D-NMR spectra, with those of previously reported, compound was evident for the characteristic 3,4-seco structure with an isopropenyl group extending from C-5. Consequently, a new 3(4)-seco structure of 12α-hydroxycyclocephagenol with an isopropenyl group extending from C-5 was established. Based on these results, the structure of **10** was established as 20,25-epoxy-6α,12α,16β,24α-tetrahydroxy-3,4-secocycloartan-4(28)-en-3-oic acid.

The effects of biotransformation products on hTERT protein levels

In preliminary screening, Western blot experiments were performed to examine the effect of biotransformation products on the hTERT protein level, which is a reverse transcriptase subunit of the telomerase enzyme. While metabolites **4** and **5** enhanced hTERT protein levels at lower concentrations as 2, 10, and 30 nM, metabolites **7**–**10** increased protein levels at 10, 30, and 100 nM concentrations—besides, metabolite **6** increased hTERT protein levels in a dose-dependent manner (Fig. 3).

Determination of telomerase enzyme activity by using TeloTAGGG Assay

After evaluating hTERT protein levels via Western Blot studies, the concentrations that increased protein levels were selected and investigated in terms of telomerase enzyme activity via Telomerase PCR ELISA assay.

Compared to the DMSO-treated control group, starting compounds and their derivatives exhibited promising telomerase activation (Fig. 4). While cyclocephagenol (**1**) increased telomerase enzyme activity at the highest concentration (300 nM) by 3.95-fold compared to DMSO, metabolites **4**, **5** and **6** improved enzyme activity as 3.89-fold (30 nM), 3.81-fold (10 nM) and 4.38-fold (300 nM), respectively. Additionally, the active dose of metabolite **2** (2.98-fold) and its derivatives **7** (5.11-fold), **8** (3.57-fold), **9** (2.74-fold), and **10** (2.90-fold) were 100 nM. The positive control, cycloastragenol, provided a 3.5-fold increase in telomerase activation at 100 nM (Fig. 4).

Discussion

The fact that telomerase activators have the potential to be used not only in anti-aging therapies but also in regenerative medicine and degenerative diseases makes them very valuable [30–35, 42, 43]. One of the significant reluctancy to apply telomerase activators in the field has been their probable action on cellular transformation to initiate cancer. In recent years, studies on the discovery of telomerase activators and their molecular/mechanistic basis have increased with the demonstration that telomerase activation via small molecules does not cause cancer [44–49]. Several natural products have been reported as telomerase activators [50–52]. Among them, cycloastragenol plays a vital role in this field as the first commercialized compound [30–35, 42, 43]. Indeed, a recent finding by Deng et al. (2022) reporting that cycloastragenol inhibits tumor growth in vivo was also entirely meaningful for the field [53].

Based on the telomerase activator potentials of cycloartanes and our previous studies [37–39], we decided to carry out biotransformation studies on cyclocephagenol (**1**), a novel cycloartane-type sapogenin from *Astragalus* species, and its 12-hydroxy derivatives. As there was no bioactivity data on cyclocephagenol and its derivatives in terms of telomerase activation, we first evaluated the hTERT protein level of cyclocephagenol (**1**) and its 12-hydroxy derivatives (**2** and **3**) on HEKn cells. While cyclocephagenol (**1**) and **3** increased hTERT protein levels in a dose-dependent manner, metabolite **2** increased these protein levels at 10, 30, and 100 nM concentrations.

Since the hTERT protein levels of these compounds were notable, biotransformation studies were carried out on cyclocephagenol and its 12-hydroxy derivatives within the scope of this study. Biotransformation studies yielded seven new biotransformation products (Fig. 2). Structural elucidations were accomplished through 1D-, 2D-NMR, and HR-ESI-MS analysis. As in our previous study, *C. laburnicola* was found to catalyze oxidation,
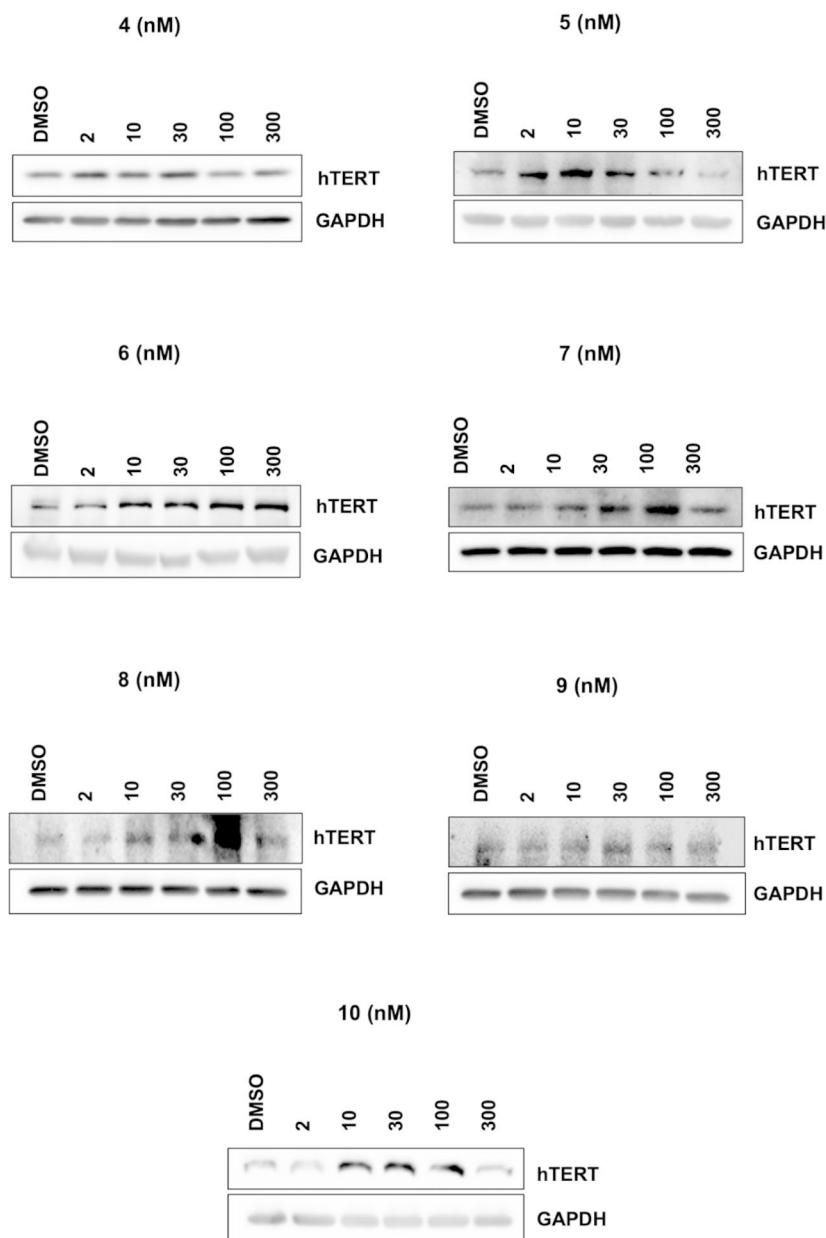
4 (nM)

hTERT
GAPDH

5 (nM)

hTERT
GAPDH

6 (nM)

hTERT
GAPDH

7 (nM)

hTERT
GAPDH

8 (nM)

hTERT
GAPDH

9 (nM)

hTERT
GAPDH

10 (nM)

hTERT
GAPDH

Fig. 3 Effects of biotransformation products (**4**–**10**) on hTERT protein level

Baeyer-Villiger oxidation, ring opening, and dehydration reactions, respectively.

A biotransformation study on cyclocephagenol (**1**) resulted in the production of three compounds (**4**: 3(4)-seco, **5**: A ring-lacto, and **6**: 3-oxo), as in the biotransformation of cycloastragenol [37, 39]. Interestingly, in the biotransformation study performed with 12α-hydroxycyclocephagenol, a dehydration reaction (**10**) was also achieved in addition to these modifications (**7**: 3-oxidation; **8**: lactone formation; **9**: 3(4)-ring cleavage). This modification was also observed in the

biotransformation of astragenol in our previous studies [37, 39].

In the continuation, biotransformation products were screened for their effects on telomerase enzyme activation, and Western Blot analysis was used for the preliminary screening. The effect of metabolites on hTERT protein level was investigated by Western Blot in the dose range of 2-300 nM. As a result, all metabolites were active compared to the DMSO-treated control group. The dose range for the TeloTAGGG study was determined as 2–30 nM for metabolites **4** and **5**, while the 30–300 nM range
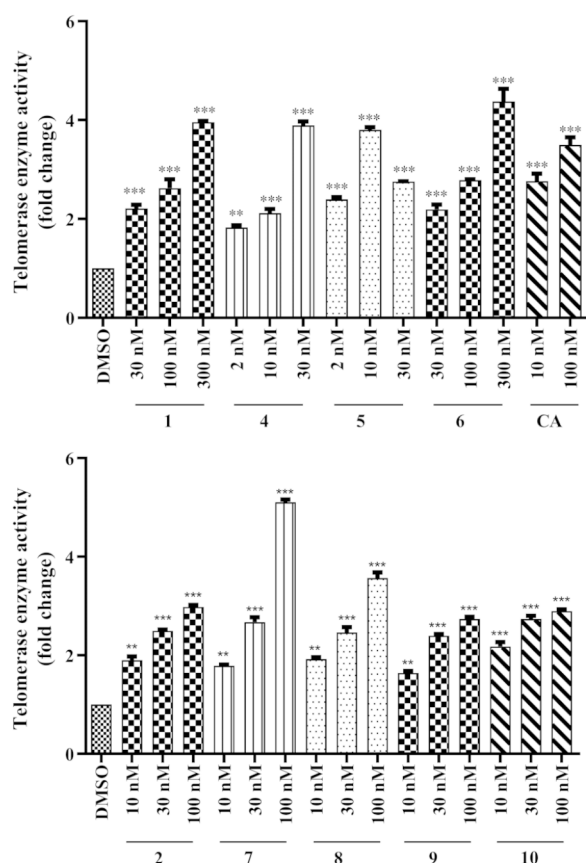
Fig. 4 Telomerase activity of **1**, **2**, **4**–**10** in cell lysates measured by Telo-TAGGG assay. Values are expressed as the fold change relative to the control DMSO. Error bars are presented as standard deviations (n = 2; *p ≤ 0.05, **p ≤ 0.001, ***p ≤ 0.005). CA: Cycloastragenol, positive control

was chosen for **1** and **6**. Metabolites **2** and **7**–**10** were tested in the 10–100 nM dose range. Additionally, the most active doses of cycloastragenol (10 and 100 nM) were preferred as the positive control.

According to TeloTAGGG results, all molecules except metabolite **5** showed dose-dependent telomerase activation compared to the control. On the other hand, metabolite **5** showed a dose-dependent increase up to 10 nM and decreased at 30 nM. In addition, the effect of metabolites on hTERT protein level was consistent with Telo-TAGGG results.

In evaluating the starting compounds (**1** and **2**), cyclocephagenol was found to be more active at a higher dose (3.96-fold at 300 nM). In comparison, metabolite **2** showed lower activity (2.98-fold) at 100 nM than cycloastragenol. The hydroxylation at C-12 caused a decrease in activity compared to our previous studies.

Metabolites **6** (4.38-fold at 300 nM) and **7** (5.11-fold at 100 nM), possessing a ketone functionality at C-3, are noteworthy because they are the most active derivatives. While hydroxylation at C-12 decreased telomerase

activation in metabolite **2** (2.98-fold at 100 nM) compared to **1** (3.96-fold at 300 nM), a more active metabolite was obtained at a lower dose when oxidation in C-3 occurred in **2** (**7**). When examining the 3-oxo derivatives from a chemical point of view, (i) the hydrogen bond donor characteristic in C-3 has disappeared and has completely switched to the acceptor position, (ii) the polarity has decreased relatively compared to the starting compound, (iii) the chair conformation has changed in the A ring, resulting in a boat conformation. Although it is premature to infer a structure-activity relationship with a limited number of compounds, the copresence of oxidation at C-3 and monooxygenation at C-12 seems to be important in increasing telomerase activation.

Metabolites **5** and **8** are formed because of Baeyer-Villiger monooxygenase activity and contain seven-membered lactones in the A ring. Metabolite **5** provided a 3.81-fold telomerase activation at 10 nM, while metabolite **8** exhibited a 3.57-fold activation at a higher dose (100 nM). Contrary to 3-oxo derivatives, the hydroxylation at C-12 causes a decrease in activity in lactone derivatives. Lactone derivatives have similar properties with 3-oxo derivatives: (i) a high electron density at the hydrogen bond acceptor position in the A ring, (ii) partial boat conformation, (iii) slightly more polar character than 3-oxo derivatives.

After lactone ring formation, a lactone hydrolase enzyme catalyzes a further step to yield 3(4)-seco metabolites (metabolites **4**, **9**, and **10**). When these three molecules were tested, it was observed that metabolite **4** showed similar activity to metabolite **1** at lower doses, but metabolites **9** and **10** did not provide an increase in telomerase activation. Metabolites **4** and **9** carrying hydroxy at C-4 showed 3.89-fold activation at 30 nM and 2.74-fold at 100 nM, respectively; metabolite **10** containing C-4(28) double bonds provided a 2.9-fold activation at a concentration of 100 nM. As with lactone derivatives, hydroxylation at C-12 caused a decrease in activity. Considering the general physicochemical properties of 3(4)-seco, its more polar and ionizable nature due to the presence of a carboxylic acid is significant, especially for water solubility and possible electrostatic interactions. The carboxylic acid formed in the A ring (C-3) and the hydroxylation at C-4 forming an electron-rich region might be the key feature for molecular interactions with biological macromolecules (membrane/nuclear receptors and/or proteins) at the cellular level.

Collectively, the tested cyclocephagenol derivatives also demonstrated potent telomerase activation compared to the positive control cycloastragenol (varying between 1.02- and 1.46-fold).

Conclusion

Based on the potent telomerase activity of *C. laburnicola* biotransformation metabolites deriving from cycloastragenol and astragenol, we made a further attempt to discover new activators. To be sure, cyclocephagenol and its 12-hydroxy derivatives were good candidates for telomerase activation, a preliminary test was performed on the hTERT protein level, revealing that both compounds were notably active. Thus, in continuation, biotransformation studies were initiated with *C. laburnicola* to give seven new molecules. As in our previous studies, *C. laburnicola* catalyzed oxidation at C-3 and ring-opening reactions by Baeyer-Villiger oxidation on the cyclocephagenol and 12α-hydroxycyclocephagenol. When the compounds were tested by TeloTAGGG assay, it was noteworthy that cyclocephagenol and its metabolites had more potency regarding telomerase activation than the positive control cycloastragenol.

Experimental

General experimental procedures

NMR spectra were obtained at 400 MHz for ^{1}H and 100 MHz for ^{13}C on a Varian Oxford AS400 spectrometer, and 600 MHz for ^{1}H and 150 MHz for ^{13}C on an Agilent 600 MHz Premium Compact in C_5D_5N with solvent peak used as a reference. Column chromatography (CC) was carried out on silica gel 60 (Merck 7734) and RP (C-18, Merck 9303). TLC analyses were carried out on Silica gel 60 F254 (Merck 5554) and RP-18 F254 (Merck) plates. Compounds were detected by UV and 20% aq. H_2SO_4 spraying reagent followed by heating at 105 °C for 1–2 min.

Microorganism and starting compound

Cyclocephagenol (**1**) was donated by Bionorm Natural Products (İzmir, Türkiye). 12α-hydroxycyclocephagenol (**2**) and 12β-hydroxycyclocephagenol (**3**) was isolated in our previous study by using *A. eureka* [40]. *C. laburnicola* used in this study was isolated from fresh and healthy leaves of *A. angustifolius*. The original strain was deposited at the Bedir Laboratory with the deposit number 20131E4BL1 [39]. All cultures were maintained on potato dextrose agar (PDA, Merck, 1.10130.0500) slants and stored at 4 °C until use. Before biotransformation, the fungus was pre-cultivated on PDA in Petri dishes for 10 days at 25 °C.

Microbial transformation procedure

Stock cultures stored at 4 °C in an agar slant were transferred to the fresh PDA medium and incubated at 25 °C for 10 days. Following incubation, Tween 80 (0.1%) was added to the fungi grown in the PDA medium, and a spore solution was obtained by scraping with an inoculation loop. The spore suspension was inoculated to potato dextrose broth (PDB, HKM Culture Media, 021053). After three days of incubation, the substrate (20 mg/mL in DMSO) was dosed at 1% (v/v) of the medium. Preparative-scale biotransformation studies were performed employing 100 mg of **1** for 4 days, 30 mg of **2** for 30 days, and 30 mg of **3** for 30 days with *C. laburnicola* (25 °C and 180 rpm).

Extraction and isolation

After an incubation period, the fungal mycelia were filtered on a Buchner funnel, and the filtrate was extracted with EtOAc (×3). The organic phase was evaporated under reduced pressure to dryness.

Compounds **4**–**6** were isolated from the EtOAc extract (120 mg) of *C. laburnicola* with **1**. This extract was subjected to vacuum-liquid chromatography (VLC) loaded with reversed-phase silica gel (RP-C18, 30 g) to yield **4** (22.6 mg), **6** (9.2 mg), and one impure fraction (A) after elution with an ACN:H_2O gradient (40:60, 50:50, 60:40, 100:0). Fraction A (7.9 mg) was chromatographed on a silica gel column (10 g) using $CHCl_3$:MeOH gradient (100:0, 98:2, 97:3) to afford 29 fractions. Fractions from A22 to A26 (6.8 mg) were combined and re-chromatographed over a silica gel column (10 g) using $CHCl_3$:IPA gradient (99:1, 97:3) to afford **5** (2.3 mg).

Compounds **7**–**10** were isolated from the EtOAc extract of **2** (241 mg) by *C. laburnicola*. This extract was chromatographed on a silica gel column (33 g) using *n*-hexane:EtOAc:MeOH:H_2O (10:10:2:0, 10:10:3:0, 0:100:17.5:13.5) gradient to give four impure fractions (Fractions A-D). Each impure fraction was subjected to vacuum-liquid chromatography (VLC) loaded with reversed-phase silica gel (RP-C18, 20 g) to yield **7** (7.2 mg), **8** (3.7 mg), **9** (3.4 mg), and **10** (2 mg).

Spectral data of 4–10

Metabolite 4: ^{1}H-NMR (C_5D_5N, 400 MHz) and ^{13}C-NMR (C_5D_5N, 100 MHz): see Tables 1 and 2; HR-ESI-MS (positive ion mode): *m/z* 545.34691 ($C_{30}H_{50}NaO_7$, calcd. 545.34487).

Metabolite 5: ^{1}H-NMR (C_5D_5N, 400 MHz) and ^{13}C-NMR (C_5D_5N, 100 MHz): see Tables 1 and 2; HR-ESI-MS (positive ion mode): *m/z* 527.33635 ($C_{30}H_{48}NaO_6$, calcd. 527.33431).

Metabolite 6: ^{1}H-NMR (C_5D_5N, 400 MHz) and ^{13}C-NMR (C_5D_5N, 100 MHz): see Tables 1 and 2; HR-ESI-MS (positive ion mode): *m/z* 511.33940 ($C_{30}H_{48}NaO_5$, calcd. 511.33939).

Metabolite 7: ^{1}H-NMR (C_5D_5N, 600 MHz) and ^{13}C-NMR (C_5D_5N, 150 MHz): see Tables 1 and 2; HR-ESI-MS (negative ion mode): *m/z* 503.33835 ($C_{30}H_{47}O_6$, calcd. 503.33781).

Metabolite 8: ^{1}H-NMR (C_5D_5N, 400 MHz) and ^{13}C-NMR (C_5D_5N, 100 MHz): see Tables 1 and 2;

Table 1 ^{1}H NMR data of compounds **4–10** (in C_5D_5N)

H	4[a] δ$_H$ (J in Hz)	5[a] δ$_H$ (J in Hz)	6[a] δ$_H$ (J in Hz)	7[b] δ$_H$ (J in Hz)	8[a] δ$_H$ (J in Hz)	9[b] δ$_H$ (J in Hz)	10[b] δ$_H$ (J in Hz)
1	1.67 m, 2.71 m	1.28 m, 1.95 m	1.25 m, 1.96 m	1.38 m, 2.11 m	1.42 m, 1.99 m	1.82 m, 2.77 m	1.80 t (13.1), 2.53 m
2	2.60 m, 2.96 m	2.60 m, 2.88 m	2.43 ddd (14.3, 8.1, 6.8), 2.70 ddd (14.2, 8.6, 5.9)	2.43 ddd (14.1, 8.4, 6.0), 2.77 m	2.58 dd (13.2, 5.1), 2.89 td (13.3, 7.0)	2.74 m, 3.00 m	2.70 m, 2.95 m
3	-	-	-	-	-	-	-
4	-	-	-	-	-	-	-
5	2.37 d (8.4)	2.40 d (9.3)	2.18 d (9.7)	2.29 d (9.8)	2.44 d (9.3)	2.45 d (8.3)	2.78 d (9.7)
6	4.05 dd (12.7, 5.6)	3.66 m	3.64 m	3.70 dd (9.9, 4.9)	3.70 m	4.10 m	3.64 m
7	1.58 m, 1.79 m	1.51 m, 1.69 m	1.58 m, 1.71 m	1.75 (2 H)	1.62 m, 1.70 m	1.72 m, 1.85 m	1.65 m, 1.90 m
8	1.59 m	1.72 m	1.86 m	1.88 m	1.72 m	1.67 m	1.94 m
9	-	-	-	-	-	-	-
10	-	-	-	-	-	-	-
11	1.15 m, 2.30 m	0.80 m, 2.02 m	0.91 m, 1.98 m	1.76 m, 2.38 m	1.67 m, 2.35 dd (14.6, 5.8)	2.04 dd (14.5, 8.4), 2.69 dd (14.5, 6.8)	2.11 m, 2.73 m
12	1.68 m, 1.84 m	1.74 m, 1.85 m	1.69 m, 1.82 m	4.26 ddd (9.2, 6.1, 2.6)	4.25 t (7.6)	4.28 t (7.9)	4.28 t (7.7)
13	-	-	-	-	-	-	-
14	-	-	-	-	-	-	-
15	1.77 m, 2.15 m	1.80 m, 2.15 m	1.79 m, 2.17 m	1.90 m, 2.19 dd (12.7, 7.9)	1.89 m, 2.21 dd (12.5, 7.8)	1.89 m, 2.23 dd (12.6, 7.7)	1.91 m, 2.21 dd (12.6, 7.9)
16	4.89 dd (13.4, 7.7)	4.68 dt (8.2, 4.2)	4.90 tdd (8.1, 5.4, 3.2)	4.93 m	4.93 m	4.93 q (7.2)	4.94 m
17	2.06 d (7.7)	2.10 d (7.7)	2.07 d (7.3)	2.97 d (8.0)	2.96 d (8.1)	2.97 d (8.3)	2.99 d (8.0)
18	1.71 s	1.70 s	1.68 s	1.71 s	1.70 s	1.76 s	1.75 s
19	0.59 d (4.4), 1.00 d (4.4)	0.53 d (5.0), 0.79 d (4.9)	0.31 d (4.1), 0.64 d (4.2)	0.48 d (4.2), 0.70 d (4.2)	0.67 d (4.8), 0.84 d (4.9)	0.74 d (4.4), 1.06 d (4.4)	0.63 d (4.4), 0.73 d (4.4)
20	-	-	-	-	-	-	-
21	1.55 s	1.60 s	1.57 s	1.99 s	1.97 s	1.98 s	1.99 s
22	1.24 m, 3.03 m	1.26 m, 3.11 m	1.24 m, 3.08 td (13.5, 4.5)	2.13 dd (13.1, 3.7)	2.10 d (13.4), 2.78 t (12.2)	2.13 m, 2.78 m	2.13 m, 2.81 m
23	1.87 m, 2.16 m	1.91 m, 2.21 m	1.87 m, 2.19 m	1.94 dd (14.0, 3.7), 2.34 t (3.4)	1.95 m, 2.35 m	1.93 m, 2.34 t (13.9)	1.94 m, 2.34 t (14.0)
24	3.66 brs	3.70 brs	3.66 brs	3.73 brs	3.72 brs	3.73 brs	3.74 s
25	-	-	-	-	-	-	-
26	1.44 s	1.47 s	1.44 s	1.57 s	1.56 s	1.58 s	1.59 s
27	1.27 s	1.32 s	1.28 s	1.39 s	1.39 s	1.40 s	1.40 s
28	1.76 s	1.93 s	1.74 s	1.78 s	1.94 s	1.80 s	5.09 s, 5.21 s
29	1.60 s	1.67 s	1.42 s	1.50 s	1.70 s	1.65 s	1.89 s
30	0.94 s	0.94 s	0.92 s	1.28 s	1.27 s	1.31 s	1.33 s

[a] 400 MHz, [b] 600 MHz, †Overlapped signals

Table 2 ^{13}C NMR data of compounds **4–10** (in C_5D_5N)

C	4[a] δ_C	5[a] δ_C	6[a] δ_C	7[b] δ_C	8[a] δ_C	9[b] δ_C	10[b] δ_C
1	31.9†	33.0	31.6	32.3	32.5	33.0	31.1
2	32.9	34.3	35.6	36.0	33.6	34.0	33.1
3	176.0	174.5	216.6	217.4	173.6	179.5	177.3
4	75.7	86.1	50.3	51.0	85.3	76.4	147.1
5	53.3	53.8	53.3	54.0	53.2	54.2	55.7
6	71.1	71.6	69.0	70.0	70.9	71.9	69.3
7	36.9	37.9	38.1	39.1	37.4	37.7	36.7
8	46.8†	48.6	47.8	49.1	48.1	47.8	49.0
9	25.0	22.3	20.9	21.8	21.7	29.2	30.7
10	28.5	26.5	28.1	28.7	25.8	25.7	22.2
11	26.5	27.1	26.0	38.6	38.2	38.7	39.0
12	34.2	34.6	33.8	74.5	73.0	74.0	73.4
13	46.9†	47.1	46.5	46.8	51.0	47.2	47.0
14	45.3	46.1	45.7	52.0	46.0	51.8	51.8
15	48.7	49.3	48.1	51.4	51.0	51.9	51.3
16	73.8	74.4	73.7	72.5	71.9	72.7	72.3
17	60.9	61.5	60.7	55.7	54.9	55.7	55.5
18	22.0	22.5	21.5	21.2	20.5	21.5	21.2
19	31.9†	31.8	30.8	31.4	30.8	32.3	32.4
20	78.8	79.5	78.8	79.9	79.3	80.0	79.8
21	28.5	29.1	28.4	27.8	27.1	27.8	27.7
22	26.4	27.1	26.4	29.4	28.6	29.2	29.1
23	23.8	24.5	23.8	24.3	23.6	24.3	24.2
24	68.4	69.1	68.4	69.2	68.5	69.3	69.1
25	75.1	75.9	75.1	76.3	75.5	76.4	76.2
26	28.4	29.1	28.4	29.1	28.4	29.1	28.9
27	27.8	28.6	27.8	28.7	28.0	28.8	28.6
28	33.3	32.4	28.4	29.3	31.7	34.0	115.3
29	28.8	28.5	20.1	20.7	27.8	29.5	20.7
30	20.7	21.5	20.4	22.6	22.1	22.6	22.3

[a] 100 MHz, [b] 150 MHz, †Overlapped signals

HR-ESI-MS (negative ion mode): *m/z* 519.33289 ($C_{30}H_{47}O_7$, calcd. 519.33272).

Metabolite 9: ^{1}H-NMR (C_5D_5N, 600 MHz) and ^{13}C-NMR (C_5D_5N, 150 MHz): see Tables 1 and 2; HR-ESI-MS (negative ion mode): *m/z* 537.34344 ($C_{30}H_{49}O_8$, calcd. 537.34329).

Metabolite 10: ^{1}H-NMR (C_5D_5N, 600 MHz) and ^{13}C-NMR (C_5D_5N, 150 MHz): see Tables 1 and 2; HR-ESI-MS (negative ion mode): *m/z* 519.33122 ($C_{30}H_{47}O_7$, calcd. 519.33272).

Bioactivity studies

Cell line and culture conditions

Primary human epidermal keratinocyte cells (HEKn) (ATCC; PCS-200-010) were cultured in Dermal Cell Basal Media (ATCC; PCS-200-030) supplemented with Keratinocyte Growth Kit (ATCC; PCS-200-040) according to the manufacturer's instructions at 37 °C under humidified 5% CO_2. HEKn cells were seeded at a density of 2500 to 5000 cells per cm^2 when they reached 70–80% confluency.

Immunoblotting studies

The lysates of cells were prepared in RIPA buffer (1% Nonidet P-40, 0.5% sodium deoxycholate, and 0.1% SDS in 1X PBS, pH 8.0) with a protease inhibitor cocktail (Roche, Switzerland). Protein concentrations were determined via BCA assay (Thermo Fisher Scientific, US). At first, equal amounts of prepared were denatured with 4X Laemmli buffer at 95 °C. Then denatured samples were loaded into gels and separated by SDS-PAGE electrophoresis. After electrophoresis was completed, gels were transferred to PVDF membranes (EMD Millipore, US, IPVH00010). After blocking membranes in 5% non-fat dry milk prepared in 1X PBS-0.1% Tween-20, membranes were labeled with primary and secondary antibodies. In this study, antibodies against hTERT (Origene, TA301588) and GAPDH (CST, 5174) were used. Secondary antibodies (Goat anti-rabbit-31460 and Goat anti-mouse-31430) were used. The proteins' chemiluminescence signals were determined with Clarity ECL substrate solution (BIORAD, US, 1705061) by Vilber

Loumart FX-7 (Thermo Fisher Scientific, US). ImageJ software (http://imagej.nih.gov/ij/) was used for Western blot images.

Telomerase activity assay

The identification of telomerase enzyme activity was performed in HEKn cells by TeloTAGGG Telomerase PCR Plus Kit (Sigma Aldrich, 12013789001) according to the supplier's instruction. The obtained data were presented as a fold change of DMSO used as a solvent control. Experiments were done in two biological experiments with two technical replicates. A one-way ANOVA Post Hoc test was used for statistical analysis of this assay using GraphPad Prism software. The significance of the differences was determined as $*p \leq 0.05$, $**p \leq 0.001$, $***p \leq 0.005$.

Supplementary Information

The online version contains supplementary material available at https://doi.org/10.1186/s12934-023-02069-3.

> **Additional file 1.** Mass and NMR spectra of biotransformation products **4-10.**

Declarations

Ethics approval and consent to participate
Not applicable.

Consent for publication
All authors approved the manuscript.

Competing interests
The authors declare no competing interests.

References
1. Bhatti HN, Khera RA. Biological transformations of steroidal compounds: a review. Steroids. 2012;77:1267–90.
2. Bureik M, Bernhardt R, Bureik M, Bernhardt R. Steroid hydroxylation: microbial steroid biotransformations using cytochrome P450 enzymes. Mod Biooxidation. 2007;155:176.
3. Carballeira JD, Quezada MA, Hoyos P, Simeó Y, Hernaiz MJ, Alcantara AR, et al. Microbial cells as catalysts for stereoselective red–ox reactions. Biotechnol Adv. 2009;27:686–714.
4. Donova MV, Egorova OV. Microbial steroid transformations: current state and prospects. Appl Microbiol Biotechnol. 2012;94:1423–47.
5. Lam KS. Application of Whole-Cell Biotransformation in the Pharmaceutical Industry. Biocatalysis for the Pharmaceutical Industry: Discovery, Development, and Manufacturing. 2009.
6. Fernandes P, Cruz A, Angelova B, Pinheiro HM, Cabral JMS. Microbial conversion of steroid compounds: recent developments. Enzyme Microb Technol. 2003;32:688–705.
7. Urlacher VB. Catalysis with cytochrome P 450 monooxygenases.Handbook of Green Chemistry: Online. 2010;1–25.
8. Borges KB, de Souza Borges W, Durán-Patrón R, Pupo MT, Bonato PS, Collado IG. Stereoselective biotransformations using fungi as biocatalysts. Tetrahedron Asymmetry. 2009;20:385–97.
9. Kar S, Sanderson H, Roy K, Benfenati E, Leszczynski J. Green Chemistry in the synthesis of Pharmaceuticals. Chem Rev. 2022;122:3637–710.
10. Mamedova RP, Isaev MI. Triterpenoids from Astragalus plants. Chem Nat Compd. 2004;40:303–57.
11. Yang LP, Shen JG, Xu WC, Li J, Jiang JQ. Secondary metabolites of the genus astragalus: Structure and biological-activity update.Chem Biodivers. 2013.
12. Pistelli LF. Secondary metabolites of genus Astragalus: Structure and biological activity.Studies in Natural Products Chemistry. 2002;27.
13. Çaliş I, Yürüker A, Taşdemir D, Wright AD, Sticher O, Luo Y, De et al. Cycloartane triterpene glycosides from the roots of Astragalus melanophrurius.Planta Med. 1997;63.
14. Yesilada E, Bedir E, Çaliş I, Takaishi Y, Ohmoto Y. Effects of triterpene saponins from Astragalus species on in vitro cytokine release.J Ethnopharmacol. 2005;96.
15. Bedir E, Pugh N, Calis I, Pasco DS, Khan IA. Immunostimulatory effects of cycloartane-type triterpene glycosides from Astragalus species. Biol Pharm Bull. 2000;23:834–7.
16. Özipek M, Dönmez AA, Çaliş I, Brun R, Rüedi P, Tasdemir D. Leishmanicidal cycloartane-type triterpene glycosides from Astragalus oleifolius.Phytochemistry. 2005;66.
17. Gariboldi P, Pelizzoni F, Tatò M, Verotta L, El-Sebakhy N, Asaad AM et al. Cycloartane triterpene glycosides from Astragalus trigonus.Phytochemistry. 1995;40.
18. Uner G, Tag O, Erzurumlu Y, Kirmizibayrak PB, Bedir E. Identification of a non-canonical necrotic cell death triggered via enhanced proteolysis by a Novel Sapogenol Derivative. Chem Res Toxicol. 2020;33:2880–91.
19. Radwan MM, El-Sebakhy NA, Asaad AM, Toaima SM, Kingston DGI. Kahiricosides II-V, cycloartane glycosides from an Egyptian collection of Astragalus kahiricus.Phytochemistry. 2004;65.
20. Khushbaktova ZA, Agzamova MA, Syrov VN, Radchenko NV, Mirsalikhova NM, Umarova FT. Influence of cycloartanes from plants of the genus Astragalus and their synthetic analogs on the contractive function of the myocardium and the activity of Na,K-ATPase.Chem Nat Compd. 1995;30.
21. Sevimli-Gür C, Onbailar I, Atilla P, Genç R, Akar N, Deliloğlu-Gürhan I et al. In vitro growth stimulatory and in vivo wound healing studies on cycloartane-type saponins of Astragalus genus.J Ethnopharmacol. 2011;134.
22. Nalbantsoy A, Nesil T, Erden S, Çalış İ, Bedir E. Adjuvant effects of Astragalus saponins macrophyllosaponin B and astragaloside VII. J Ethnopharmacol. 2011;134:897–903.
23. Genç R, Yakuboğullari N, Nalbantsoy A, Çöven F, Bedir E. Adjuvant potency of astragaloside vii embedded cholesterol nanoparticles for H3N2 influenza vaccine.Turkish Journal of Biology. 2020;44.
24. Yakuboğulları N, Genç R, Çöven F, Nalbantsoy A, Bedir E. Development of adjuvant nanocarrier systems for seasonal influenza A (H3N2) vaccine based on Astragaloside VII and gum tragacanth (APS).Vaccine. 2019;37.
25. Harley CB, Chin AC, Akama T, Ip NY, Wong Y, Miller-Martini DM. Compositions and methods for increasing telomerase activity. United States; 2004.
26. De Lange T, Shelterin. The protein complex that shapes and safeguards human telomeres.Genes Dev. 2005.
27. Blackburn EH. Switching and signaling at the telomere.Cell. 2001.
28. Allsopp RC, Vaziri H, Patterson C, Goldstein S, Younglai EV, Futcher AB et al. Telomere length predicts replicative capacity of human fibroblasts. Proc Natl Acad Sci U S A. 1992;89.

29. de Jesus BB, Schneeberger K, Vera E, Tejera A, Harley CB, Blasco MA. The telomerase activator TA-65 elongates short telomeres and increases health span of adult/old mice without increasing cancer incidence.Aging Cell. 2011;10.

30. Dow CT, Harley CB. Evaluation of an oral telomerase activator for early age-related macular degeneration - A pilot study.Clinical Ophthalmology. 2016;10.

31. Harley C. Telomerase Therapeutics for Degenerative Diseases.Curr Mol Med. 2005;5.

32. Jäger K, Walter M. Therapeutic targeting of telomerase. Genes (Basel). 2016.

33. Le Saux CJ, Davy P, Brampton C, Ahuja SS, Fauce S, Shivshankar P et al. A Novel Telomerase Activator Suppresses Lung Damage in a Murine Model of Idiopathic Pulmonary Fibrosis.PLoS One. 2013;8.

34. Harley CB, Liu W, Blasco M, Vera E, Andrews WH, Briggs LA et al. A natural product telomerase activator as part of a health maintenance program. Rejuvenation Res. 2011;14.

35. Wang J, Liu Y, Xia Q, Xia Q, Wang B, Yang C et al. Potential roles of telomeres and telomerase in neurodegenerative diseases.Int J Biol Macromol. 2020.

36. Liu T, Ullenbruch M, Choi YY, Yu H, Ding L, Xaubet A et al. Telomerase and telomere length in pulmonary fibrosis.Am J Respir Cell Mol Biol. 2013;49.

37. Küçüksolak M, Ekiz G, Duman S, Yılmaz S, Ballar-Kırmızıbayrak P, Bedir E. Telomerase activators derived from Astragalus sapogenins via biotransformation with the recently discovered endophytic fungus Camarosporium laburnicola. 67th International Congress and Annual Meeting of the Society for Medicinal Plant and Natural Product Research (GA) in cooperation with the French Society of Pharmacognosy AFERP. © Georg Thieme Verlag KG; 2019.

38. Duman S, Ekiz G, Yılmaz S, Yusufoglu H, Kırmızıbayrak PB, Bedir E. Telomerase activators from 20 (27)-octanor-cycloastragenol via biotransformation by the fungal endophytes. Bioorg Chem. 2021;109:104708.

39. Ekiz G, Yllmaz S, Yusufoglu H, Klrmlzlbayrak PB, Bedir E. Microbial Transformation of Cycloastragenol and Astragenol by Endophytic Fungi Isolated from Astragalus Species.J Nat Prod. 2019;82.

40. Küçüksolak M, Üner G, Ballar-Kırmızıbayrak P, Bedir E. Neuroprotective metabolites via fungal biotransformation of a novel sapogenin, cyclocephagenol. Sci Rep. 2022;12:1–15.

41. Bedir E, Kula C, Öner Ö, Altaş M, Tağ Ö, Öngen G. Microbial transformation of Astragalus sapogenins using Cunninghamella blakesleeana NRRL 1369 and Glomerella fusarioides ATCC 9552. J Mol Catal B Enzym. 2015;115:29–34.

42. Liu J, Gao D, Dan J, Liu D, Peng L, Zhou R et al. The protective effect of cycloastragenol on aging mouse circadian rhythmic disorder induced by d-galactose.J Cell Biochem. 2019;120.

43. Wu J, Zeng Z, Li Y, Qin H, Zuo C, Zhou C et al. Cycloastragenol protects against glucocorticoid-induced osteogenic differentiation inhibition by activating telomerase.Phytotherapy Research. 2021;35.

44. Andrews NP, Fujii H, Goronzy JJ, Weyand CM. Telomeres and immunological diseases of aging.Gerontology. 2010.

45. Prescott JC, Blackburn EH. Telomerase: Dr Jekyll or Mr Hyde?Curr Opin Genet Dev. 1999;9.

46. Funk WD, Wang CK, Shelton DN, Harley CB, Pagon GD, Hoeffler WK. Telomerase expression restores dermal integrity to in vitro-aged fibroblasts in a reconstituted skin model.Exp Cell Res. 2000;258.

47. Cawthon RM, Smith KR, O'Brien E, Sivatchenko A, Kerber RA. Association between telomere length in blood and mortality in people aged 60 years or older.Lancet. 2003;361.

48. Harley CB. Telomerase is not an oncogene.Oncogene. 2002;21.

49. Thomas M, Yang L, Hornsby PJ. Formation of functional tissue from transplanted adrenocortical cells expressing telomerase reverse transcriptase.Nat Biotechnol. 2000;18.

50. Jacczak B, Rubiś B, Totoń E. Potential of naturally derived compounds in telomerase and telomere modulation in skin senescence and aging.Int J Mol Sci. 2021.

51. Kuru G, Üner G, Bedir E. Is telomerase a hidden player? Therapeutic potential of natural telomerase activators against age-related diseases.Phytochemistry Reviews. 2022.

52. Aydin Y, Orta-Yilmaz B. The role of telomerase activators in antiaging strategies and their clinical potential. Emerging anti-aging strategies. Singapore: Springer Nature Singapore; 2023. pp. 227–42.

53. Deng G, Zhou L, Wang B, Sun X, Zhang Q, Chen H et al. Targeting cathepsin B by cycloastragenol enhances antitumor immunity of CD8 T cells via inhibiting MHC-I degradation.J Immunother Cancer. 2022;10.

Publisher's Note